Journal of Colloid and Interface Science 435 (2014) 105–111

Contents lists available at ScienceDirect

Journal of Colloid and Interface Science

www.elsevier.com/locate/jcis

Polyol synthesis of silver nanocubes via moderate control of the reaction atmosphere

Seog-Jin Jeon [a], Jae-Hwang Lee [b], Edwin L. Thomas [a,*]

[a] Department of Materials Science and NanoEngineering, Rice University, Houston, TX 77005, USA
[b] Department of Mechanical and Industrial Engineering, University of Massachusetts Amherst, Amherst, MA 01003, USA

ARTICLE INFO

Article history:
Received 28 May 2014
Accepted 21 August 2014
Available online 30 August 2014

Keywords:
Polyol synthesis
Silver nanocubes
Reaction atmosphere

ABSTRACT

Silver nanocubes were successfully synthesized at high yield in variously controlled reaction atmospheres by balancing etching of O_2/Cl^- and reduction of glycolaldehyde. There have been efforts to control the O_2 content in reaction atmospheres by purging of O_2 or Ar gas for the balancing, but we found that moderate control of reaction atmosphere, just by careful timing of the opening and the capping of the reaction vial, greatly enhanced reproducibility. Enhanced reproducibility is attributed to alleviation of evaporation and condensation of glycolaldehyde (b.p. = 131 °C) by using capping at reaction temperatures higher than the b.p. of glycolaldehyde rather than purging with gas. The most important finding is that seeding is initiated by HNO_3 induced deoxygenation reaction in the gas phase. O_2 is consumed by oxidation of NO generated from the silver etching reaction by HNO_3, which effectively controls the reaction atmosphere without introduction of gas. Our simple method to control reaction atmosphere reduces the overall reaction time to one fifth of the previous result and provides excellent size and distribution selectivity of the Ag nanocube product.

1. Introduction

Silver nanomaterials have received considerable attention in the past decade due to their morphology-dependent electronic, catalytic and plasmonic properties [1–3]. Their synthesis was extensively studied by Xia and coworkers with approaches established for obtaining finely tuned unique morphologies such as cubes [4–16], wires [17–19], prisms [20,21], decahedrons [22], octahedrons [23], and bipyramids [24]. Among the various morphologies, nanocubes have been of great interest because of applications exploiting localized surface plasmon resonance (LSPR) [25–31]. Polyol synthesis is a promising method to attain high quality silver nanocubes with high yield and can be classified into two methods. One utilizes silver reduction by glycolaldehyde [5,6,9] and the other utilizes Na_2S- or NaHS-mediated reaction [7,8,10–12]. The former needs extra time for selective seed etching (SSE) for the removal of twinned seeds which otherwise result in nanowires and nanobipyramids. Several approaches have been suggested for SSE such as oxidative etching with O_2/Cl^- [5,32], etching by Fe species such as $Fe(acac)_3$ or $Fe(NO_3)_3$ [15], dissolution by HNO_3 [6], and their combinations [12].

Although there are several useful approaches for SSE, the glycolaldehyde based reaction has been utilized less than the Na_2S- or NaHS-mediated reaction due to the extremely long time for SSE over 15 h [5,6,18]. Because the time when seeding is initiated is determined by the competition between the etching action of O_2/Cl^- and the reducing action of glycolaldehyde, seeding can be considerably delayed regardless of degree of SSE, if etching overwhelms reduction. So, to shorten the SSE time, a solid understanding of how to balance etching and reduction is necessary. There are two possible approaches for balancing etching and reduction. One is to control the etching ability by the amount of O_2 and Cl^- added and the other is to control the reducing ability by changing the reaction temperature to control the conversion from ethylene glycol to glycolaldehyde, a major reducing agent [9]. For the latter, Skrabalak et al. reported that the amount of glycolaldehyde increased slightly with increase in temperature from 140 °C to 150 °C but it increased over 3 times when the temperature increased from 150 °C to 160 °C [9]. This suggests the control of the reducing ability by temperature alone will not be easy due to the non-linear relationship. On the other hand, the former can be achieved by introduction of gas. Taguchi et al. introduced O_2 gas at 160 °C [16] and Zhang et al. introduced Ar gas at 150 °C for the purpose of balancing [10]. However, one must be careful with the introduction of gas since it accelerates evaporation and condensation of both of ethylene glycol and glycolaldehyde, because

* Corresponding author. Fax: +1 713 348 5300.
E-mail address: elt@rice.edu (E.L. Thomas).

http://dx.doi.org/10.1016/j.jcis.2014.08.039
0021-9797/

the reaction temperature is above the boiling point of glycolaldehyde (b.p. = 131 °C). According to the LaMer model, uniform reduction during reaction determines the quality of nanoparticles especially at the seeding step [33]. But introduction of gas above at the boiling point of the reducing agent, glycolaldehyde, will result in fluctuations in the local concentration of the reducing agent during the seeding, leading to non-uniform seeding and irreproducible results. Also temperature differences in the reaction solution due to introduction of gas also can lead to poor results because success in polyol based Ag nanoparticle synthesis requires a reaction temperature difference <5 °C [1]. Here, we demonstrate a simple and moderate method that can readily change the atmospheric condition from O_2 abundant to O_2 rarefied *without introduction of gas* and discuss how the change in reaction atmosphere enables the successful synthesis of high quality silver nanocubes and enhancement of product reproducibility. We suggest a working hypothesis for controlling atmospheric condition, especially for the O_2 concentration, and describe a new procedure for optimizing reaction conditions.

2. Materials and methods

2.1. Synthesis

Ethylene glycol (EG, Cl < 5 ppm and Fe < 0.2 ppm, Macron Fine Chemicals), hydrochloric acid (HCl, 37%, ACS reagent, Aldrich), silver nitrate ($AgNO_3$, ⩾ 99.0%, ACS reagent, Aldrich), polyvinylpyrrolidone (PVP, Mw = 55,000, Aldrich), nitric acid (HNO_3, 70%, ACS reagent, Aldrich), and sodium chloride (NaCl, ⩾ 99.0%, ACS reagent, Aldrich) were used as received. A 22 ml vial and Teflon coated spin bar (15.9 mm × 6.4 mm) were purchased from VWR international. Ultra high purity grade oxygen and argon gas were purchased from Matheson.

2.1.1. Synthesis via moderate control of the reaction atmosphere (open-cap method)

1 ml of EG is preheated for 10 m as the reaction vial is kept open and 50 μl of 60 mM (3 μmol) HCl solution in EG is added into the vial. We used fresh HCl solution prepared within 10 h for reproducibility. After 3 m, 1 ml of 0.2 M (200 μmol) $AgNO_3$ solution in EG is injected into the vial in 20 s. After another 3 m, 1 ml of 0.12 M (120 μmol) PVP solution in EG is added in 20 s. After the duration that the vial is kept open, T_{open}, the vial is capped. Seeding starts after some time duration, T_{deox}, and full growth is completed in 35 m. The product is quenched in water bath at room temperature for 20 m and washed with acetone once and with distilled water at least three times. T_{open} is varied between 0 and 6 h. HCl volume is varied between 25 (1.5 μmol) and 100 μl (6 μmol) and PVP concentration is varied between 0.02 M (20 μmol) and 0.30 M (300 μmol). After the reaction, a spin bar is immersed in HNO_3 for an hour to dissolve silver contaminants and washed with copious amount of distilled water and dried in an oven. For HNO_3 and NaCl injection experiments, 25 ml of 60 mM (1.5 μmol) of HNO_3 and 75 ml of 60 mM (4.5 μmol) NaCl solution in EG are used. All other conditions are same but time intervals between HNO_3 injection and NaCl injection and between NaCl injection and $AgNO_3$ injection are 1 m and 2 m, respectively. Stirring speed for all experiments is 900 rpm for the efficient gas exchange.

2.1.2. Synthesis via gas introduction

For O_2 and Ar introduction experiments, a glass pipet is used to introduce a continuous flow of gas above the reaction solution. O_2 gas is introduced right after the addition of PVP followed by Ar purging or capping of the vial. The flow rate is fixed to 150 ml/min. Reactant contents are 50 μl of 60 mM (3 μmol), 1 ml of 0.2 M (200 μmol), and 1 ml of 0.12 M (120 μmol) for HCl, $AgNO_3$, and PVP, respectively.

2.2. Characterization

Average size of nanocubes and the number of nanocubes and nanowires of at least 500 particles were analyzed by imaging software (Image-Pro) from SEM images. Based on this data, the standard deviation in size of nanocubes and $d_{w/c}$ were calculated.

The SEM images were taken using a field-emission microscope (FEI Quanta 400) operated at an accelerating voltage of 10–20 kV. High magnification images of nanocubes were taken in order to observe edge truncation at an accelerating voltage of 30 kV.

3. Results and discussion

We used $AgNO_3$ as a precursor, PVP as a stabilizer, HCl as an additive, and EG as a solvent in which the content of Cl and Fe impurities (as specified by the vendor) is under 5 ppm and 0.2 ppm, respectively. This system has been reported before by Im et al. for the synthesis of silver nanocubes without control of reaction atmosphere [6]. We use their procedure as a reference system to compare the results of our reaction via controlled reaction atmosphere. At first, HCl generates AgCl and HNO_3 as shown in reaction (1) as described by Im et al.

$$HCl + AgNO_3 \rightarrow HNO_3 + AgCl \quad (1)$$

Formation of HNO_3 and AgCl is advantageous for obtaining nanocubes. Recently it has been reported from a time-resolved X-ray diffraction study by Peng et al. [14,15,34] that AgCl is converted to seeds for nanocubes and HNO_3 promotes SSE as described by Im et al. [6] and Fievet et al. [35] Interestingly, HNO_3 is continuously regenerated as described in reactions 2–4 as illustrated in Scheme 1.

$$4HNO_3 + 3Ag \rightarrow 3AgNO_3 + NO + 2H_2O \quad (2)$$

$$2NO + O_2 \rightarrow 2NO_2 \quad (3)$$

$$3NO_2 + H_2O \rightarrow 2HNO_3 + NO \quad (4)$$

All other reactants are regenerated as illustrated by the yellow arrows in Scheme 1 but only O_2 is not regenerated as illustrated by the red arrow in Scheme 1. Our strategy is to utilize the deoxygenation reaction for fine control of O_2 in the reaction batch. If we cap the reaction vial, the O_2 concentration gradually decreases, which causes a decrease in the etching ability while the reducing ability is gradually increased by buildup of glycolaldehyde. When the reducing ability overwhelms the etching ability after a certain time, the seeding will be initiated. We define the time between capping the vial and initiation of seeding as T_{deox}, the time for deoxygenation. T_{deox} was measured by recording the time after capping at which the color of the reaction batch changed to clear yellow as shown in Fig. S2. T_{deox} linearly decreased with increase in the amount of HNO_3 as shown in Fig. S1 at the rate of 7 min/mole. Further details of the HNO_3 injection experiment are given at the end of the discussion section.

The total reaction for nanocube synthesis is comprised of three steps as shown in scheme S1. In step one, we preheated the EG as the vial is left open only for 10 min to avoid unwanted buildup in the amount of glycolaldehyde and added chemical reagents. During the second step, the vial is just left open for SSE and all of reactions including deoxygenation, seeding, and growth are done after capping the reaction vial, which is the reaction step in scheme S1. Seeding starts coincident with a yellow color after 64 min of T_{deox} with growth occurring for an additional 35 min. During growth,

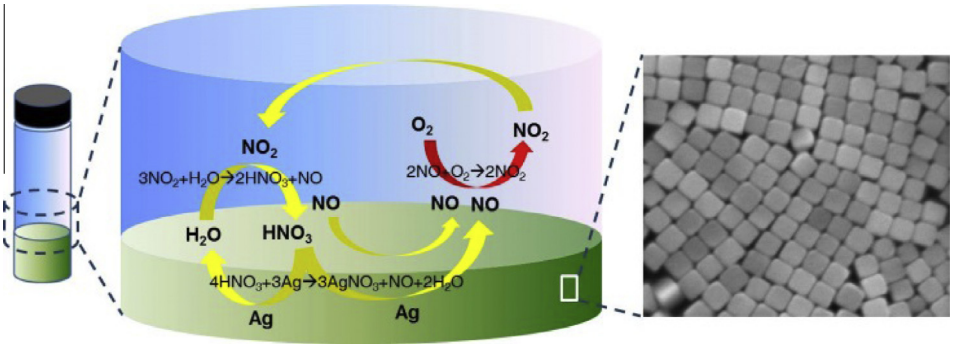

Scheme 1. Working hypothesis for deoxygenation process.

the color of the reaction solution changes from yellow to red to green-ocher to ocher as shown in Fig. S2. To control the degree of SSE, we varied the duration that the vial is kept open, T_{open}, from 0 to 6 h and provide details of reactant concentrations in the supporting materials. As T_{open} increases, the number of nanowires is decreased until T_{open} = 4 h as shown in Fig. 1a–c. To quantitatively compare the amount of nanowires, we measured the ratio of nanowire number to that of nanocubes, $d_{w/c}$, as summarized in Table 1. The minimum $d_{w/c}$ was nearly zero for T_{open} = 4 h. This observation shows that SSE effectively progressed during T_{open} and twinned seeds are almost all removed within 4 h. For longer T_{open}, most of particles become nearly spherical and smaller due to severe etching and some nanowires reappear. Dissolved Ag ions due to severe etching might lead to another round of seeding which can be the reason why nanowires reappeared. Relative to previous results [5,6] our reaction time is drastically reduced to 4 h of SSE and 95 min of growth, attributed to the precisely controlled reaction atmosphere: e.g. for Ref. [5], it took 44 h of SSE time followed by 2 h of growth time and for Ref. [6], it took 15 h of SSE time and 11 h of growth time.

To make sure the effect of abundance or lack of O_2 on seeding and as a comparative study, we introduced O_2 gas into reaction vial through a glass pipette instead of leaving the vial open and introduced Ar gas instead of capping the vial with same reactant concentrations for open-cap vial condition. During O_2 introduction, seeding and growth were not observed in an hour as for the open vial condition while, after Ar introduction for about 30 min, the reaction mixture color changed from transparent to yellow as the Ag particles started growing similar to the open-cap vial experiment. However, T_{deox} was reduced to half of the open-cap vial condition because deoxygenation by Ar gas is more direct and faster than by the reaction and consequently, the result for O_2-Ar purging experiment was not as good as the open-cap vial condition as shown in Fig. S3a. Most of the particles remained very small in size and some 105 nm nanocubes were observed due to the excess etching ability and the nonhomogeneous local concentration of glycolaldehyde inside the vial. And a large amount of nanowires was observed ($d_{w/c}$ = 0.54), attributed to the complete depletion of O_2 [5]. We also tried a different set of experiment involving the introduction of O_2 gas instead of leaving the vial open and

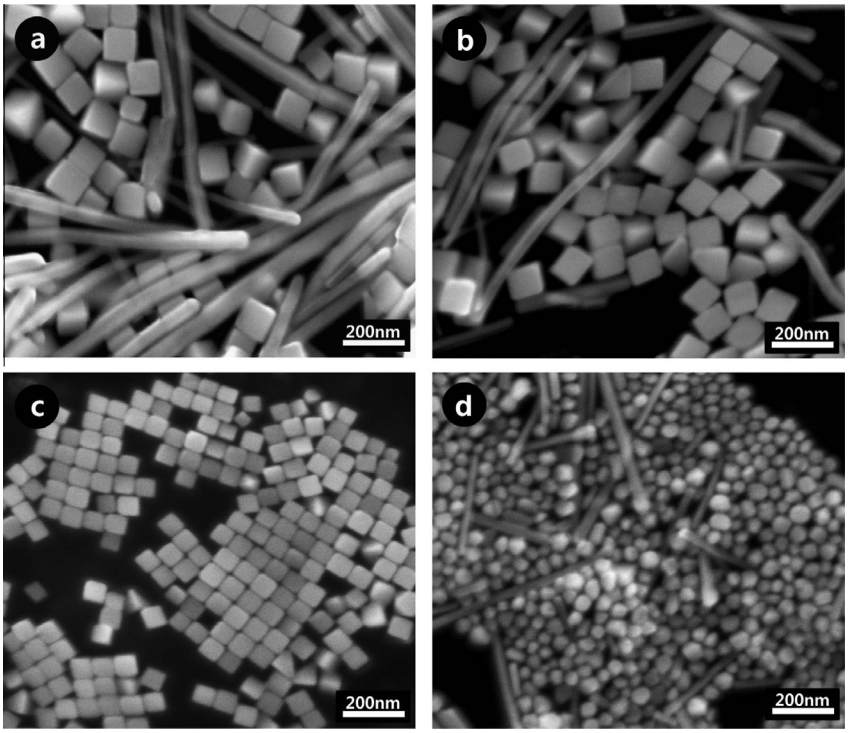

Fig. 1. SEM images of synthesized nanocubes for different T_{open}, (a) 0 h, (b) 2 h, (c) 4 h, and (d) 6 h, when the contents of HCl, $AgNO_3$, and PVP are 3, 200, and 120 μmol.

Table 1
Nanocube size and $d_{w/c}$ for various reaction atmosphere control experiments.

Atmosphere control	Size	$d_{w/c}$	Reactant contents
Vial open 0 h and capped	112 nm	0.82	HCl 3 μmol,$AgNO_3$ 200 μmol, PVP 120 μmol
Vial open 2 h and capped	108 nm	0.15	
Vial open 4 h and capped	78 nm	0.00	
Vial open 6 h and capped	50 nm	0.05	
O_2 1 h and Ar	*105 nm	0.54	
O_2 10 min and vial capped	58 nm	0.23	

* Size only for cubes not for smaller particles.

capping the vial but all particles were severely etched due to too high etching ability despite the reduced O_2 introduction duration (10 min) as shown in Fig. S3b. Therefore, we can assume that the optimized atmospheric condition is in a certain balanced region between O_2 rarefied and abundant state but the excess etching ability makes the balancing nontrivial. Our moderate control of reaction atmosphere is a more desirable route to reach the balanced region, which results in highly reproducible products as demonstrated by ten consecutive reaction batches (see Table S1).

As expected from reactions 2–4, the initial concentration of HNO_3 is the most important factor determining the amount of O_2 remaining in the seeding step. To investigate the effect of the initial concentration of HNO_3, the amount of HCl added was controlled from 1.5 μmol to 6 μmol. We found that T_{deox} is 64 min for addition of 1.5 and 3 μmol but the time is shortened to 45 min for 4.5 and 6 μmol of HCl. For the addition of 1.5 μmol of HCl, non-uniform size nanocubes were observed (Fig. 2a), while for 3 μmol, highly monodisperse nanocubes were obtained (Fig. 2b). This result corresponds with the result of Im et al. where for HCl concentrations less than the optimized one, they also observed a broadened size distribution [6]. To compare the dispersion in size between nanocubes synthesized at different hydrochloric acid content, we define the $f_{\Delta a/a}$ as the standard deviation in size, Δa, over the average size, a. The values for all runs are summarized in Table 2 along with the relative amount of HCl/$AgNO_3$/PVP. If we add more HCl (4.5 and 6 μmol), the size of the nanocubes slightly increases and {1 1 1} facets shown in scheme S2 are observed along with some smaller sized particles and nanowires. This result also corresponds well with the result of Im et al. In their work, for HCl concentrations above the optimized one, the formation of nanowires was significant. The results can be explained by the effect of the amount of HNO_3 remaining in the seeding step. If the initial amount of HCl is below 3 μmol, there is still an excess amount of O_2 due to insufficient amounts of an O_2 scavenger, HNO_3, so an excessive oxidative etching action creates non-uniformity in product size. If the initial concentration of HNO_3 is higher, the O_2 is almost all consumed and, as a result, nanowires appear because oxidative etching is very weak at seeding [5].

To investigate the detailed shape of the nanocubes, high magnification SEM images are shown as insets in Fig. 2. Edge sharpness of nanocubes for 1.5 and 3 μmol is maintained, but the apexes of nanocubes using 4.5 and 6 μmol of HCl were truncated, attributed to a higher etching ability due to an excessive amount of HNO_3. The ratio between areas of the {1 1 1} and {1 0 0} facets were 0.024 and 0.033 for the addition of 4.5 and 6 μmol of HCl, respectively. It is important to point out that very small differences in the amount

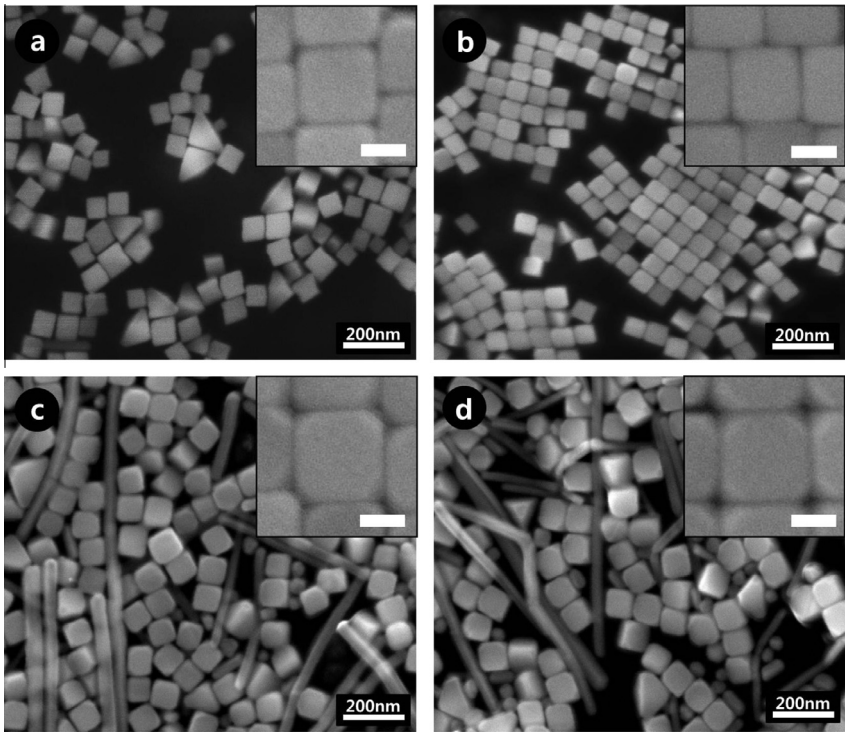

Fig. 2. SEM images of nanocubes synthesized for different HCl concentrations. HCl added are (a) 1.5, (b) 3.0, (c) 4.5, and (d) 6.0 μmol. Insets are high magnification images of nanocubes to emphasize corner truncation ({1 1 1} facets). Scale bars in insets are 50 nm.

Table 2
Size (a), standard deviation (Δa), $f_{\Delta a/a}$, and $d_{w/c}$ of nanocubes according to different HCl, $AgNO_3$, and PVP contents.

HCl/$AgNO_3$/PVP	Size (a)	(Δa)	$f_{\Delta a/a}$	$d_{w/c}$
1.5/200/120 μmol	73.0 nm	8.76	0.120	0.00
3.0/200/120 μmol	77.9 nm	4.71	0.060	0.00
4.5/200/120 μmol	91.5 nm	6.40	0.070	0.13
6.0/200/120 μmol	96.2 nm	5.65	0.062	0.21
3.0/200/20 μmol	108.9 nm	9.27	0.085	0.00
3.0/200/300 μmol	75.3 nm	4.57	0.061	0.49

of HCl used (<1.5 μmol) results in global effects on the shape of nanocubes, their size dispersion, and the occurrence of nanowires. This also means that a small change in the O_2 content brings a big change in the resultant silver products.

If the correct atmospheric condition is provided, then the reaction is solely dependent on the concentration of PVP. For the molar ratio of PVP to silver, R, of 0.1 (20 μmol of PVP), truncated nanocubes were observed together with larger, irregularly shaped Ag particles as shown in Fig. 3a. The truncation of nanocubes synthesized at a lower concentration of PVP was reported previously [36] and the appearance of larger, irregularly shaped Ag particles suggests that there is insufficient stabilization of the particle surface with PVP. As R increases, the uniformity in particle size and shape was enhanced and uniform size nanocubes were obtained at $R = 0.6$ (120 μmol of PVP) as shown in Fig. 2b. But for $R = 1.5$ (300 μmol of PVP), nanocubes were observed together with nanowires ($d_{w/c} = 0.31$) as shown in Fig. 3b. We speculate that the reason for the appearance of nanowires is an excessive amount of PVP that will accelerate reduction due to PVP's role as a reducing agent [9]. Therefore, our optimal condition for R was 0.6, a value lower than any previously reported [4–15].

There have been earlier reports about the production of silver nanocubes via control of the reaction atmosphere. Taguchi et al. reported synthesis of 200 nm nanocubes at a specific O_2 flow rate at 160 °C [16] and Zhang et al. showed that Ar atmosphere was good for obtaining high quality nanocubes without nanowires at 150 °C [10]. In both experiments, we can assume that the amount

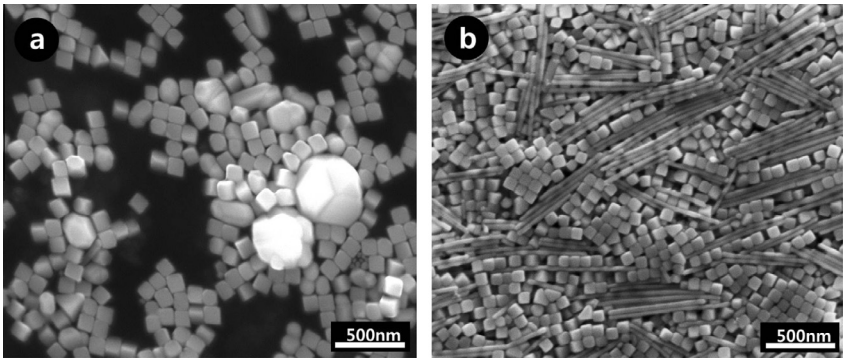

Fig. 3. SEM images of nanocubes synthesized at different molar relative ratio R of PVP to $AgNO_3$. (a) $R = 0.1$ and (b) $R = 1.5$.

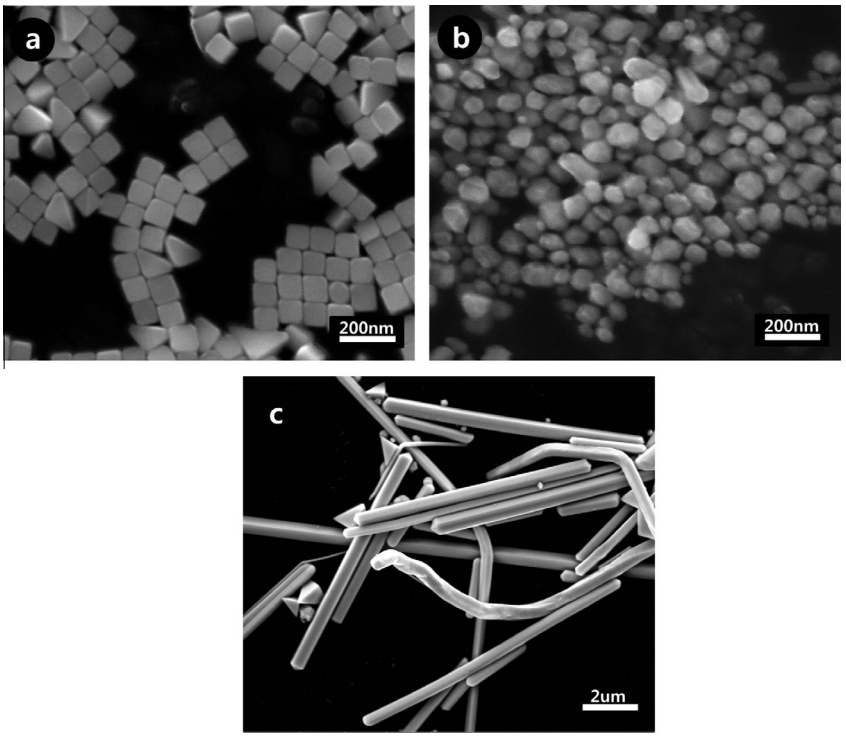

Fig. 4. SEM images of (a) nanocubes synthesized with the injection of 1.5 μmol of HNO_3 and 4.5 μmol of NaCl, (b) severely truncated nanocubes with the injection of 1.5 μmol of HNO_3, and (c) large wires with bipyramids with the injection of 4.5 μmol of NaCl.

of glycolaldehyde was already sufficient for the reduction of silver at starting point of reaction because EG was preheated for 1 h, however, the totally different glycolaldehyde situation for both experiments can be explained by the nearly three times greater generation of glycolaldehyde at 160 °C than at 150 °C as reported by Skrabalak et al. [9]. For the result of Taguchi et al., the enormously strengthened reducing ability due to accelerated generation of glycolaldehyde at 160 °C will need higher etching ability of pure O_2 to reach optimized region between reducing and etching ability. But, rapid evaporation of glycolaldehyde due to the high reaction temperature, 30 °C higher than boiling point of glycolaldehyde (131 °C), and forced condensation by gas introduction will cause severe fluctuations in local concentration of glycolaldehyde inside the reaction solution, which will result in non-uniform reducing ability from batch to batch. Thus, it seems difficult to reproducibly reach the same balance point between extremely strong etching by pure O_2 and variable reducing actions by the fluctuating glycoaldehyde concentration. For the result of Zhang et al., though their reaction temperature is 10 °C lower than that of Taguchi et al., the flow rate of Ar is much higher, 1200 ml/min but this high gas flow rate will likely lead to fluctuations in glycolaldehyde concentration. However, it seems that the use of Na_2S or NaHS has a positive role in the overall reaction. Zhang et al. recognized the need for different atmospheres for the selective etching step and the growth step, but they did not address the key role of each reaction atmosphere. Instead, they developed approaches circumventing the effect of the gas species. For example, they introduced a new silver precursor, CF_3COOAg [11,12], instead of $AgNO_3$ to exclude the generation of NO and NO_2 gas during the reaction. But this involves a drastic increase in production cost. And it is also hard to practically weigh the exact amount of Na_2S or NaHS due to their hygroscopic nature, though the reaction is quite sensitive to very small variations in their concentration [8]. On the other hand, the simplicity in reactants makes our reaction cost-effective and reproducible.

The interplay between the role of HNO_3 and Cl^- by controlling the amount of HNO_3 and NaCl independently is worth further examination and we hope to find several balance points between the amount of HNO_3 and Cl^- for obtaining similar quality nanocubes introduced in this report. For example, nanocubes synthesized by the injection of both 1.5 μmol of HNO_3 and 4.5 μmol of NaCl were similar to the best result in this report as shown in Fig. 4a. But only severely truncated nanocubes (Fig. 4b) or products with a lot of large wires with a small number of bipyramids (Fig. 4c) were observed by the single injection of either 1.5 μmol of HNO_3 or 4.5 μmol of NaCl, respectively. So, it is clear that the role of both HNO_3 and NaCl is important in the synthesis of silver nanocubes. It also should be noted that T_{deox} linearly decreased with increase in the amount of HNO_3 added for the single HNO_3 injection experiment as shown in Fig. S1. As described in reactions 2–4, the amount of HNO_3 is directly related to the deoxygenation rate. For 3.2 μmol of HNO_3 (53 μl of 60 mM), T_{deox} was 62 min but it decreased to 37 min with the addition of 6.8 μmol (113 μl of 60 mM). The error bar in Fig. S1 is ± 1 min. The rate of T_{deox} decrease according to the mole of HNO_3 was 7 min/μmol and this is direct evidence of the role of HNO_3 as an O_2 scavenger.

4. Conclusions

In summary, we have successfully synthesized high quality silver nanocubes by precise control of O_2 in the reaction atmosphere by simply opening and capping the reaction vial. When the reaction vial is left open during T_{open}, twinned seeds are selectively removed and when the vial is capped, reaction was initiated after some time duration (T_{deox}) for deoxygenation. 4 h of T_{open} was sufficient for complete removal of nanowires, which resulted in high quality nanocubes with an edge length of 80 nm and low dispersity ($f_{\Delta a/a}$) of 0.06 for optimized reactant concentrations. Our approach greatly reduced the reaction time to one fifth the previous result of Im et al., which is attributed to precise control of reaction atmosphere by deoxygenation. Deoxygenation occurs by regeneration of HNO_3 through the reactions 2–4, which was evidenced by the relations between the amount of HNO_3 and T_{deox}. T_{deox} linearly decreased with the increase in the amount of HNO_3 and the rate of decrease was 7 min/mole. In this reaction, deoxygenation was controlled by the amount of HCl and T_{deox} was 64 min for the optimized condition. As compared with gas introduction experiments, the moderate control of O_2 via opening and capping the vial showed enhanced product quality. Moreover, our method is shows enhanced reproducibility over 10 consecutive batches by preventing the fluctuation of glycolaldehyde concentration. The best result from the HCl injection also could be reproduced by the separate injection of HNO_3 and NaCl and this means the each role of both HNO_3 and Cl^- is important for the reaction. Our work shows the importance of the understanding the role of reaction atmosphere in polyol synthesis of silver nanomaterials. A firm understanding makes the reaction simple, cost-effective, and highly reproducible. Scale-up should be possible with a similar volume ratio of reaction atmosphere to reactant mixture by employing better gas exchange condition between the atmosphere and a larger volume of reactant fluid by rigorous stirring.

Acknowledgment

This work was supported by AOARD grants 114095 and 114078 by DTRA under contract 1-12-1-0008.

Appendix A. Supplementary material

Supplementary data associated with this article can be found, in the online version, at http://dx.doi.org/10.1016/j.jcis.2014.08.039.

References

[1] M. Rycenga, C.M. Cobley, J. Zeng, W. Li, C.H. Moran, Q. Zhang, D. Qin, Y. Xia, Chem. Rev. 111 (2011) 3669.
[2] M.R. Jones, K.D. Osberg, R.J. Macfarlane, M.R. Langille, C.A. Mirkin, Chem. Rev. 111 (2011) 3736.
[3] Y. Xia, Y. Xiong, B. Lim, S.E. Skrabalak, Angew. Chem. Int. Ed. 48 (2009) 60.
[4] Y. Sun, Y. Xia, Science 298 (2002) 2176.
[5] B. Wiley, T. Herricks, Y. Sun, Y. Xia, Nano Lett. 4 (2004) 1733.
[6] S.H. Im, Y.T. Lee, B. Wiley, Y. Xia, Angew. Chem. Int. Ed. 44 (2005) 2154.
[7] A.R. Siekkinen, J.M. McLellan, J. Chen, Y. Xia, Chem. Phys. Lett. 432 (2006) 491.
[8] S.E. Skrabalak, L. Au, X. Li, Y. Xia, Nat. Protoc. 2 (2007) 2182.
[9] S.E. Skrabalak, B.J. Wiley, M. Kim, E.V. Formo, Y. Xia, Nano Lett. 8 (2008) 2077.
[10] Q. Zhang, C. Cobley, L. Au, M. McKiernan, A. Schwartz, L.-P. Wen, J. Chen, Y. Xia, ACS Appl. Mater. Interfaces 1 (2009) 2044.
[11] Q. Zhang, W. Li, L.-P. Wen, J. Chen, Y. Xia, Chem. Eur. J. 16 (2010) 10234.
[12] Q. Zhang, W. Li, C. Moran, J. Zeng, J. Chen, L.-P. Wen, Y. Xia, J. Am. Chem. Soc. 132 (2010) 11372.
[13] Y. Ma, W. Li, J. Zeng, M. McKiernan, Z. Xie, Y. Xia, J. Mater. Chem. 20 (2010) 3586.
[14] S. Peng, Y. Sun, Chem. Mater. 22 (2010) 6272.
[15] S. Peng, J.S. Okasinski, J.D. Almer, Y. Ren, L. Wang, W. Yang, Y. Sun, J. Phys. Chem. C 116 (2012) 11842.
[16] A. Taguchi, S. Fujii, T. Ichimura, P. Verma, Y. Inouye, S. Kawata, Chem. Phys. Lett. 462 (2008) 92.
[17] Y. Sun, B. Mayers, T. Herricks, Y. Xia, Nano Lett. 3 (2003) 955.
[18] B. Wiley, Y. Sun, Y. Xia, Langmuir 21 (2005) 8077.
[19] K.E. Korte, S.E. Skrabalak, Y. Xia, J. Mater. Chem. 18 (2008) 437.
[20] R. Jin, C. Cao, C.A. Mirkin, K.L. Kelly, G.C. Schatz, J.G. Zheng, Science 2001 (1901) 294.
[21] Y. Xiong, A.R. Siekkinen, J. Wang, Y. Yin, M.J. Kim, Y. Xia, J. Mater. Chem. 17 (2007) 2600.
[22] B. Pietrobon, V. Kitaev, Chem. Mater. 20 (2008) 5186.
[23] A. Tao, P. Sinsermsuksakul, P. Yang, Angew. Chem. Int. Ed. 45 (2006) 4597.
[24] B.J. Wiley, Y. Xiong, Z.-Y. Li, Y. Yin, Y. Xia, Nano Lett. 6 (2006) 765.
[25] L.J. Sherry, S.-H. Chang, G.C. Schatz, R.P. Van Duyne, B.J. Wiley, Y. Xia, Nano Lett. 5 (2005) 2034.

[26] S.Y. Lee, L. Hung, G.S. Lang, J.E. Cornett, I.D. Mayergoyz, O. Rabin, ACS Nano 4 (2010) 5763.
[27] N. Grillet, D. Manchon, F. Bertorelle, C. Bonnet, M. Broyer, E. Cottancin, J. Lermé, M. Hillenkamp, M. Pellarin, ACS Nano 5 (2011) 9450.
[28] M. Rycenga, X. Xia, C.H. Moran, F. Zhou, D. Qin, Z.-Y. Li, Y. Xia, Angew. Chem. Int. Ed. 50 (2011) 5473.
[29] B. Gao, G. Arya, A.R. Tao, Nat. Nanotechnol. 7 (2012) 433.
[30] M.A. Mahmoud, M. Chamanzar, A. Adibi, M.A. El-Sayed, J. Am. Chem. Soc. 134 (2012) 6434.
[31] A. Moreau, C. Ciracì, J.J. Mock, R.T. Hill, Q. Wang, B.J. Wiley, A. Chilkoti, D.R. Smith, Nature 492 (2012) 86.
[32] Y. Xiong, J. Chen, B. Wiley, Y. Xia, J. Am. Chem. Soc. 127 (2005) 7332.
[33] V.K. LaMer, R.H. Dinegar, J. Am. Chem. Soc. 72 (1950) 4847.
[34] C. Goessens, D. Schryvers, J. Van Landuyt, R. De Keyzer, Ultramicroscopy 40 (1992) 151.
[35] F. Fievet, J.P. Lagier, M. Figlarz, MRS Bull. 14 (1989) 29.
[36] X. Xia, J. Zeng, L.K. Oetjen, Q. Li, Y. Xia, J. Am. Chem. Soc. 134 (2012) 1793.